

Fig. 4. The coincidence between K-conversion electrons of the 244 keV transition and gamma rays harder than 500 keV.

← Fig. 2. The electron spectrum of ^{152}Eu and ^{154}Eu sources.

Coincidences were recorded between the K-conversion line of the 244.7 keV transition feeding the 121.78 keV level and the K- or L-conversion line of the 121.78 keV transition. Figure 1 shows the decay scheme of ^{152}Eu .

The electron spectrum of $^{152}\text{Eu} + ^{154}\text{Eu}$ sources obtained in our spectrometer is shown in Figure 2. It is clear that the 123 keV transition of ^{154}Gd overlaps with the 122 keV transition of ^{152}Sm , and the 248 keV transition of ^{154}Gd with the 244.7 keV transition of ^{152}Sm , so the lifetime of the 123 keV level in ^{154}Gd will contribute in our measurements.

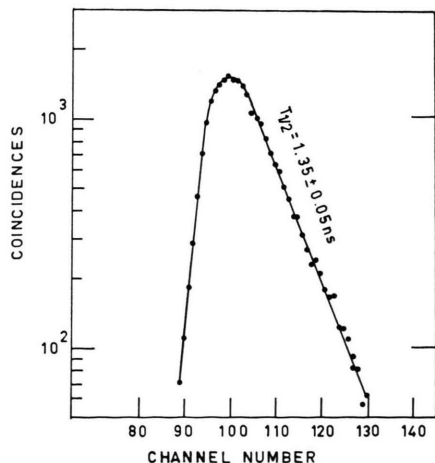


Fig. 3. The delayed curve obtained for the 122 keV level.

As the average weighted mean value for 5 selected runs, and after correction for the admixtures⁶, taking the value $T_{1/2} = (1.18 \pm 0.04)$ ns⁷ for the 123 keV level of ^{154}Gd , a value of $T_{1/2} = (1.35 \pm 0.05)$ ns is obtained for the 121.78 keV level in ^{152}Sm . Figure 3 shows the delayed curve obtained for the 121.78 keV level in ^{152}Sm .

Lifetime of the 366.5 keV level in ^{152}Sm

Measurements were carried out using the comparison technique as described in Ref. 6. Coincidences were recorded between the gamma transitions of energies greater than 500 keV feeding the 366.5 keV level and the K-conversion electrons of the 244 keV transition. The prompt curves for comparison were taken using a ^{60}Co source. Several runs were taken and the weighted mean value corrected for admixtures from the 371 keV level of ^{154}Gd with $T_{1/2} = (41 \pm 7)$ ps⁷.

A value of (42 ± 18) ps is obtained for the half-life of the 366.5 keV level in ^{152}Sm . Coincidences obtained for the 366.5 keV level are shown in Figure 4.

III. Discussion

Table 1 summarizes the experimental results for determining the half-lives of the 121.78 and 366.5 keV levels in ^{152}Sm . Some reported values of the half-life of the 121.78 keV level in ^{152}Sm ^{8,9} agree with our value of (1.35 ± 0.05) ns. The other values¹⁰⁻¹² agree within the overlapping error limits.

Table 1.

Level	$T_{1/2}$	Authors
122 keV	(1.40 ± 0.1) ns	SUNYAR ⁸
	(1.37 ± 0.04) ns	FOSSAN ⁹
	(1.45 ± 0.06) ns	BIRK ¹⁰
	(1.43 ± 0.04) ns	HÜBNER ¹¹
	(1.45 ± 0.03) ns	DIAMOND ¹²
	(1.35 ± 0.05) ns	Present Work
366 keV	80 ps	ALKHAZOV ¹³
	(59 ± 2) ps	DIAMOND ¹²
	(42 ± 18) ps	Present Work

The half-life of the 366.5 keV level in ^{152}Sm was measured by Coulomb excitation ¹³, and recently by the Doppler shift method ¹². Our value of $T_{1/2} = (42 \pm 18)$ ps agrees very well with the value obtained by the Doppler shift method. The value obtained by Coulomb excitation is higher than the other values. By considering the 121.78 keV and 244.7 keV transitions as pure electric quadrupole transitions, we deduced the reduced transition probabilities experimentally from the measured mean lives τ_m using the formula

$$[B(E2)_{\text{rad.}}]^{-1} = 1.23 \times 10^{-2} E^5 (1 + \alpha_{\text{tot}}) \tau_m$$

where E is in keV, $B(E2)$ in units of $e^2 10^{-48} \text{ cm}^4$ and τ_m in sec.

$B(E2; 2+ \rightarrow 0+)$ is the radiative reduced transition probability, which differs from

$B(E2; 0+ \rightarrow 2+)$ obtained from Coulomb excitation by a factor of 5. In general

$$B(E2; I_i \rightarrow I_{f,\text{rad.}}) = [(2I_f + 1)/2(I_i + 1)] \cdot B(E2; I_f \rightarrow I_i)_{\text{c.exc.}}$$

In determining the experimental transition probabilities we used the experimental values for τ_m , the theoretical values for the internal conversion coefficients α_K and α_L ¹⁴, and the sum of the coefficients of the higher shells

$$(\alpha_M + \alpha_N + \dots) = 0.315 \alpha_L.$$

The experimental transition probabilities were compared with the transition probabilities in terms of the single particle model; the enhancement factors are shown in Table 2.

$$\text{The ratio } \frac{B(E2; 4+ \rightarrow 2+)_{\text{exp.}}}{B(E2; 2+ \rightarrow 0+)_{\text{exp.}}} = 1.863 \pm 0.4,$$

obtained experimentally seems to be higher than the value of 1.43 given by Bohr and Mottelson in the unified nuclear model with axial symmetry.

One can calculate the reduced transition probability predicted by the asymmetric rotator of the DAVYDOV and CHABAN model ⁴. In this model the parameter (γ) determines the deviation of the shape of the nucleus from axial symmetry. This parameter can be deduced by two methods:

$$(i) \quad \frac{E_\gamma(2+)}{E_1(2+)} = \frac{3 + \sqrt{9 - 8 \sin^2(3\gamma)}}{3 - \sqrt{9 - 8 \sin^2(3\gamma)}}.$$

$E_1(2+)$ represents the energy of the first $2+$ excited state, $E_\gamma(2+)$ represents the energy of the $(2+)$ state in the γ -vibrational band.

(ii) From the ratio: $E_1(4+)/E_1(2+)$, the energies of the first and second excited states in the ground rotational band ¹⁵.

Method (i) gives the values

$$\gamma = 15.2^\circ \quad \text{and} \quad \frac{B(E2; 4+ \rightarrow 2+)}{B(E2; 2+ \rightarrow 0+)} = 1.326.$$

Method (ii) gives the values

$$\gamma = 22.1^\circ \quad \text{and} \quad \frac{B(E2; 4+ \rightarrow 2+)}{B(E2; 2+ \rightarrow 0+)} = 2.13.$$

The reduced transition probability given by method (ii) is preferred to be compared with the experimental value.

The electric quadrupole moments Q_0 of a nuclear state are calculated according to the formula ¹⁶

$$B(E2; I_i \rightarrow I_f) = \frac{5}{16\pi} e^2 Q_0^2 (I_i 2 K 0 | I_f 2 I_f k)^2$$

for an E2 transition between successive levels in a rotational spectrum, which depends on the nuclear shape.

The nuclear deformation parameter, β , is calculated for ^{152}Sm for a transition between states of $I+2 \rightarrow I$ from the formula ⁸

$$T_\gamma = 2.18 \cdot 10^8 A^{1/3} E^5 Z^2 \beta_\tau^2 \frac{(I+1)(I+2)}{(2I+3)(2I+5)}$$

where E is measured in units MeV.

For the moments of inertia (Table 2), if we assume that the nucleus exhibits a rigid rotation, a value of $I_{\text{rig}} = 28.97 (10^{-39} \text{ keV s}^2)$ is deduced ³ for its rigid moment of inertia. This value is higher than the value $I = 11.14 (10^{-39} \text{ keV s}^2)$ of a symmetric rotor deduced from the first excited state of the nucleus. On the other hand, if the nucleus is assumed to exhibit an irrotational motion, its moment of inertia ³ will be $I_{\text{irr}} = 2.4 (10^{-39} \text{ keV s}^2)$ which is much smaller than the moment of inertia of a

Table 2.

Nucleus	State	Transition Energy (keV)	$T_{1/2}$ Present Work	$B(E2)$ $e^2 10^{-48} \text{ cm}^4$	$Q_0 10^{-24} \text{ cm}^2$	β	I keV s ² 10 ⁻³⁹	$I_{\text{rig.}}$ keV s ² 10 ⁻³⁹	$I_{\text{irr.}}$ keV s ² 10 ⁻³⁹	Enhancement Factor
¹⁵² ₆₂ Sm ₉₀	2+	121.78	(1.35 ± 0.05) ns	0.737 ± 0.027	6.084	.318	11.14	28.97	2.4	215
	4+	244	(42 ± 18) ps	1.373 ± .6	8.304	.360	5.54	29.29	3.04	271

symmetric rotator. The contribution of the rigid and the irrotational part of the motion depends on the nuclear deformation parameter β . When the de-

formation is small, only the irrotational motion will dominate and when the deformation is large only the rigid motion will dominate.

¹ M. GOLDBABER and A. W. SUNYAR, Phys. Rev. **83**, 906 [1951].

² J. RAINWATER, Phys. Rev. **79**, 432 [1950].

³ A. BOHR and B. R. MOTTELSON, Dan. Mat. Fys. Medd. **27**, No. 16 [1953].

⁴ A. S. DAVYDOV and A. A. CHABAN, Nucl. Phys. **20**, 499 [1960].

⁵ T. R. GERHOLM and J. LINDSKOG, Ark. Fys. **24**, 171 [1963].

⁶ Z. AWWAD, O. E. BADAWY, M. R. EL-AASSER, and A. H. EL-FARRASH, in Course of Publication.

⁷ J. LINDSKOG and T. SUNDSTROM, Ark. Fys. **24**, 199 [1963].

⁸ A. W. SUNYAR, Phys. Rev. **98**, 653 [1955].

⁹ D. B. FOSSAN and B. HERSKIND, Nucl. Phys. **40**, 24 [1963].

¹⁰ M. BIRK, G. GOLDRING, and Y. WALFSON, Phys. Rev. **116**, 730 [1959].

¹¹ A. HÜBNER, Z. Physik **183**, 25 [1965].

¹² R. M. DIAMOND, F. S. STEPHENS, R. NORDHAGEN, and K. NAKAI, Phys. Rev. C **3**, (No. 1), 344 [1971].

¹³ D. G. ALKHAZOV, Bull. Acad. Sci. USSR **28**, 146 [1964].

¹⁴ R. S. HAGER and E. C. SELTZER, Internal Conversion Tables, Calt 63-60 AEC Research and Development Report.

¹⁵ R. B. MOORE and C. WHITE, J. Physics **38**, 1149 [1960].

¹⁶ K. ALDER, A. BOHR, T. HUUS, B. MOTTELSON, and A. WINTHER, Rev. Mod. Phys. **28**, 432 [1956].

Relaxation of Diffused Zinc Atoms During Short-Range-Ordering in Cu-30% Zn Alloy

T. H. YOUSSEF

National Research Centre, Dokki, Cairo

(Z. Naturforsch. **27** a, 1232—1234 [1972]; received 4 April 1972)

The internal friction which is a diffusion dependent physical property has been used as a means to determine the kinetics of short range order in (Cu-30% Zn) alloy. Curves of relative (Q^{-1}/Q_0^{-1}) against annealing time have been plotted for various annealing temperatures. An average activation energy of 1.7 eV was found for the ordering process, which is equal to the activation energy for zinc diffusion in coarse grained copper.

When an alloy having short range order (SRO), is quenched from high temperatures, excess vacancies are liberated which will enhance diffusion, and hence the ordering rate during subsequent annealing. Due to this enhanced ordering rate, the equilibrium degree of short range order can be achieved in reasonable times even at rather low temperatures, provided that vacancies are mobile at these temperatures. For copper-zinc alloys in the alpha phase, the existence of SRO has been theoretically¹ established and experimentally demonstrated by many workers (cf. CLAREBROUGH et al.²). Evidence from diffuse X-ray and/or neutron scattering experiments is not available because of the small difference in scattering power of copper and zinc³ atoms. Long

range order in alpha brass above -30°C is improbable³ because of the rather low ordering energy of the system.

1. Experimental Procedure and Results

Internal friction experiments were carried out using a torsion pendulum (test wire dia. 1 mm, length 6 cm). The free decay of the oscillations was observed at frequency 0.7 c/sec and strain amplitude 1×10^{-4} . The torsion pendulum is kept at 2×10^{-5} mm Hg vacuum.

Specimens used were prepared from high purity copper and zinc. The appropriate proportions of the two components were melted in closed graphite molds mechanically agitated for homogenization. The solid solutions were cold drawn into wires of 1 mm diameter. Subsequent chemical analysis allowed the precise de-